Electrical Resistivity of Epitaxial Au Films Surface-Modulated by Arrays of Pt Nanoparticles

Gerd Kästle,[a] Alexander Schröder,[a] Hans-Gerd Boyen,[a] Alfred Plettl,[a] Paul Ziemann,[a] Oliver Mayer,[b] Joachim Spatz,*[b,c] Martin Möller,[b,d] Michael Büttner,[e] and Peter Oelhafen[e]

Keywords: Thin films / Gold / Conductivity / Platinum nanoparticles

Arrays of Pt nanoparticles with a high degree of hexagonal short-range order are deposited by means of self-assembly of diblock-copolymers on top of high quality epitaxial Au films and their influence on the electrical properties is studied. The temperature-dependent resistivity of the nanomodulated Au films is surprisingly well described by the classical size effect model of Fuchs–Sondheimer, which is based on a mixture of diffuse and specular surface scattering events. Especially, no specific influence of the interparticle distance of the nanoparticle array could be detected even though it was of the same magnitude as the elastic mean free path of the scattering electrons. Rather, the nanomodulation acts as randomly distributed scatterers leading to an overall decreased probability for specular reflections of conduction electrons at the sample surface.

Introduction

When sample dimensions are reduced as in thin films, surfaces become increasingly important having a strong impact on many of the sample properties like, e.g. electrical conductivity. Although it was speculated already one century ago[1] that the resistivity of thin metal films should deviate from the resistivity of corresponding bulk samples, it was only about 40 years later that Fuchs[2] and Sondheimer,[3] respectively, first developed models to describe the size effect of the electrical resistivity in thin films quantitatively. Along with continuous improvements of the experimental conditions (e.g. purification of starting materials, vacuum technology, analytical tools), sophisticated experiments revealed a large variety of interesting aspects.[4–25]

Common to all of these experiments were either epitaxially grown films with surfaces as flat as possible or polycrystalline films with a finite surface roughness representing a statistical distribution of the film thickness. The influence of a well-defined highly-ordered surface roughness, however, on the electrical resistivity of thin films has not yet been examined. In such a case, it could be speculated that the temperature-dependent resistivity should show deviations from the usually observed behavior whenever the electron mean free path would be a multiple of the characteristic distance between the artificial surface structures.

With the recent developments of powerful methods to produce ensembles of nanostructures on flat surfaces with a high degree of hexagonal short-range order and the individual nanostructures having dimensions approaching the Fermi wavelength of metals (typically some few nanometers), such a study has now become possible. In this work, thin metal films are patterned with a simple bottom-up technique based on molecular self-assembly.[26,27] Arrays of chemically clean Pt nanoparticles are prepared with a diameter of about 3 nm and an interparticle distance of about 30 nm. With these nanoparticles, it is possible to prepare nanomodulated thin metal films with a modulation length comparable to the mean free path of the electrons. The nanomodulated metal films have to fulfill several requirements to be suitable for such transport measurements: First, the metal film itself must be thin enough to ensure the necessary surface sensitivity of the resistivity. Second, it must be epitaxially grown without a magnetic seedlayer to minimize electron scattering within the film as well as additional spin scattering at the film/substrate interface, and third it must be chemically inert because of ex situ steps which are needed for the preparation of the metallic nanoparticles. Finally, the film has to be flat to guarantee that transport properties are governed by the nanomodulation and not by the intrinsic surface roughness of the sample. All these requirements are met by epitaxial Au films grown on sapphire with a Nb seedlayer.[28]

[a] Abteilung Festkörperphysik, Universität Ulm, 89069 Ulm, Germany
[b] Abteilung Organische Chemie III, Universität Ulm, 89069 Ulm, Germany
[c] Present address: Biophysical Chemistry, University of Heidelberg, INF 253, 69120 Heidelberg, Germany
[d] Present address: Deutsches Wollforschungsinstitut, Veltmannplatz 8, 52062 Aachen, Germany
[e] Institut für Physik, Universität Basel, Klingelbergstr. 82, 4056 Basel, Switzerland

Results and Discussion

Size Effect of the Electrical Resistivity

The temperature dependence of the electrical resistivity in bulk metals is described by the Bloch–Grüneisen relation [Equation (1)].

$$\rho_{bulk} = \rho_{0,bulk} + K\left(\frac{T}{\theta_D}\right)^5 \int_0^{\theta_D/T} \frac{x^5 dx}{\left(e^x - 1\right)\left(1 - e^{-x}\right)} \quad (1)$$

Here θ_D is the Debye temperature, K is a material specific factor and $\rho_{0,bulk}$ is the residual resistivity. The electron mean free path due to impurities l_{imp} is related to the residual resistivity by $\rho_{0,bulk} = m \cdot v_{Fermi}/n \cdot e^2 \cdot l_{imp}$. For thin films, however, with a thickness approaching l_{imp}, scattering of the electrons at the surface can no longer be neglected. In the classical size effect model by Fuchs–Sondheimer (FS),[3] surface scattering is included and the resistivity of thin films ρ_{film} can be deduced from the resistivity of the bulk metal [Equation (2)].

$$\frac{\rho_{bulk}}{\rho_{film}} = 1 - \frac{3}{2\kappa} \int_0^1 du \cdot \left(u - u^3\right) \frac{(1-p)\left(1 - e^{-\kappa/u}\right)}{1 - p \cdot e^{-\kappa/u}} \quad (2)$$

Here $\kappa = t/l$ is the ratio between film thickness t and the electron mean free path l in the bulk metal. The so-called specularity parameter p, describes phenomenologically the surface scattering of the electrons. Complete specular scattering corresponds to $p = 1$ whereas complete diffuse scattering corresponds to $p = 0$.

Transport Measurements

Before investigating the influence of a controlled nanomodulation with nanoparticles on the electrical resistivity of the Au films, the resistivity of as-prepared Au films without artificial roughness needs to be addressed, which has been done in a recent study.[23] The high epitaxial quality and the small roughness of the Au films allowed a detailed analysis of the temperature dependence of the resistivity for film thicknesses even down to 2 nm. Surprisingly, the experimental data could be described best within the framework of the classical Fuchs–Sondheimer model[3] while an analysis based on the more physically motivated models of Mayadas–Shatzkes or Soffer[5] gave results that are not physically relevant. Further investigations on medium energy ion irradiated films also confirmed this finding.[24] None of the experiments performed on epitaxially grown Au films gave any hint of a strong influence of the Nb seedlayer on their transport properties. In addition, due to the small thickness of this layer (1 nm), its transition into the superconducting state was found to be suppressed. Furthermore, despite the high quality of the Au films, no influence of quantum effects on the resistivity could be observed and only the original classical size effect model was able to consistently describe the experimental results. Thus, it seems to be justified to analyze the resistivity of the present nanomodulated Au films within the framework of the Fuchs–Sondheimer model.

Nanomodulation of the Film Surface Using Pt Nanoparticles

Arrays of Pt nanoparticles with a high degree of hexagonal short-range order were deposited on top of epitaxially grown Au films (as described in more detail in the experimental section) serving as scattering centers for the conduction electrons. A slight increase in statistical roughness at the Au film surface can be expected due to the plasma treatment[29] necessary to remove organic precursors. However, since all of the preparation procedures have been performed simultaneously on both the nanomodulated as well as the reference film, all sample properties should be identical except for the nanomodulation. Thus, in case of any resistivity changes due to, e.g., the plasma-induced roughening at the surface, this effect will be present in both the nanomodulated as well as the reference Au film.

Figure 1 shows atomic force microscopy (AFM) pictures of an epitaxially grown Au film (thickness t = 25 nm) with one half serving as a reference film (parts a and b in Figure 1) and the other half being nanomodulated with Pt nanoparticles on its surface (parts c and d in Figure 1). Even though the combination of oxygen and hydrogen

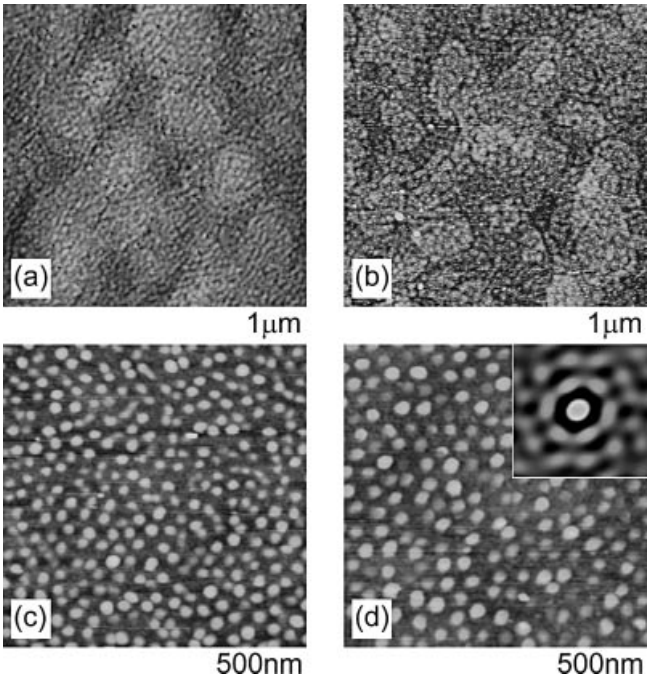

Figure 1. AFM images of the Au reference sample (a, b: z scale 3 nm) and the sample modulated with Pt nanoparticles (c, d: z scale 10 nm). The images were taken after polymer removal by the oxygen plasma (a, c) and after reduction of a thin Au oxide layer (thickness = 4 nm[29]), which is formed in the oxygen plasma by applying an additional hydrogen plasma step (b, d).

plasmas, which is required for the nanoparticle deposition, leads to a finite film roughness of the reference film of 0.23 nm_{rms} (Figure 1, a) and 0.28 nm_{rms} (Figure 1, b), respectively, the underlying terrace structure of the epitaxial Au film is still visible. After the oxygen plasma treatment, the Pt nanoparticles (Figure l, c) have a spacing of about 32 nm and a height of 3.7 nm, which is reduced to 2.9 nm by the subsequent hydrogen plasma (Figure 1, d). This decrease is due to the reduced nanoparticle volume in the metallic state as compared to the oxidized state, resulting from the exposure to an oxygen plasma. Although not perfectly ordered, the final nanoparticle arrangement exhibits a high degree of hexagonal short-range order as evidenced by the corresponding autocorrelation function shown in the inset of Figure 1 (d). Thus, deviations from the usually observed surface scattering effects induced by a statistical (random) surface roughness[4–25] can indeed be expected.

It has to be emphasized that it is not at all self-evident that stable metallic nanoparticles can be prepared on top of metal films. For Ag clusters, it was found that the clusters dissolve on epitaxial Ag films for temperatures $T > 300$ K whereas they are stable for $T < 225$ K.[30] Although Pt and Au are known to be fully miscible in the bulk, the diffusion constant turns out to be too small for Pt atoms to diffuse from the nanoparticles into the underlying Au film. Assuming a maximum temperature of 80 °C (required for the final conditioning of the nanomodulated sample, see below) which will be kept for a period of 3 days, a diffusion length $L = \sqrt{D \cdot t}$ of well below the interatomic distance can be estimated from published data for the diffusion constant $D = D_0 \cdot e^{-E/k_B T}$ with $D_0 = 9.5 \times 10^{-6}$ $m^2 s^{-1}$ and $E = 2.09$ eV.[31]

This estimate can experimentally be verified by means of X-ray Photoelectron Spectroscopy (XPS). Figure 2 (a) displays the Pt–4f core level spectrum (open symbols) of a nanomodulated sample acquired after annealing to about 80 °C in order to get rid of adsorbed water followed by an additional hydrogen plasma step in order to remove hydrocarbon adsorbates (see below). The Pt–4f spectrum can be well described by fitting[32] a single doublet (solid line) to the data using Doniach–Sunjic type line shapes.[33] As can be recognized in Figure 2 (a), the experimental binding energy position of the Pt–$4f_{7/2}$ core level agrees well with the value measured under identical conditions on a Pt reference sample (vertical solid line), but disagrees with published data[34] for the chemical shift observed in Pt_xAu_{100-x} intermetallic compounds (dashed line: $Pt_{75}Au_{25}$; dotted line: $Pt_{50}Au_{50}$; dash-dotted line: $Pt_{25}Au_{75}$). It is worth mentioning that the size of the final Pt nanoparticles (2.9 nm) matches the information depth of the spectroscopy (twice the photoelectron mean free path corresponding to 3 nm). Thus, significant intermixing between the Pt nanoparticles and the Au substrate can safely be excluded.

In addition to the binding energy position, the analysis of the line shape also provides valuable information about the electronic structure of the nanoparticles, which due to their reduced size of less than 3 nm, could be expected to show molecular/insulating rather than metallic properties. As can be seen in part a of Figure 2, the experimental core level spectrum exhibits a significant asymmetry towards higher binding energies (corresponding to lower kinetic energies of the outgoing photoelectrons) reflecting the creation of electron-hole pairs during photoemission in the vicinity of the Fermi energy E_F. This large asymmetry clearly indicates a high density of states at E_F[35] and, consequently, provides evidence that a particle size of about 3 nm is still large enough to maintain metallic properties of the nanodots allowing a strong coupling to the conduction electrons of the underlying Au film.

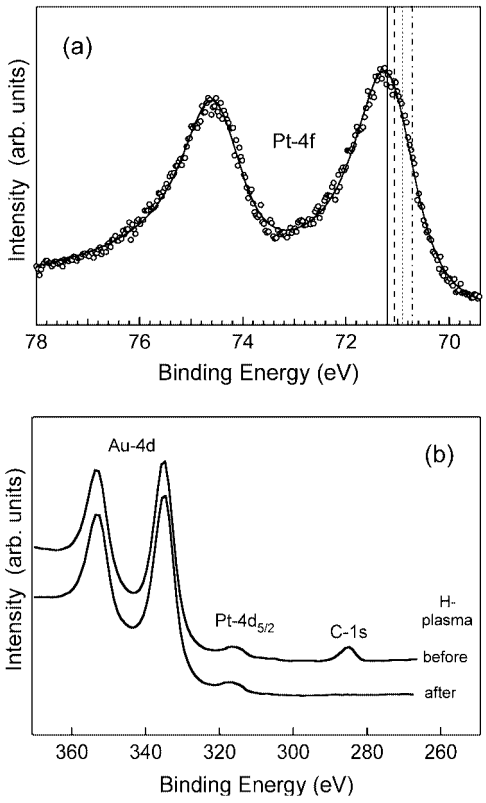

Figure 2. XPS core level spectrum of the Pt–4f doublet acquired after the final H-Plasma step (a) and C-ls binding energy range before and after annealing to about $T = 80$ °C followed by a hydrogen plasma treatment in order to remove adsorbates from the film surface (b). The vertical lines in (a) indicate the position of the Pt–$4f_{7/2}$ core level measured on a Pt reference sample (solid line) as well as the chemical shift observed for Pt_xAu_{100-x} intermetallic compounds[34] (dashed line: $Pt_{75}Au_{25}$, dotted line: $Pt_{50}Au_{50}$, dash-dotted line: $Pt_{25}Au_{75}$).

Surface Sensitivity

Because the resistivity of very thin metallic layers is strongly influenced by surface scattering of the conduction electrons special care has been taken in order to minimize the influence of adsorbates[4,10] like water or hydrocarbons which will accumulate at the surface when exposing the samples to ambient conditions and to various solvents required to perform the lithographic steps. In Figure 3, the resistivity $\rho_{4\,K}$ measured at $T = 4$ K (which corresponds to the residual resistivity ρ_0) and the room temperature resis-

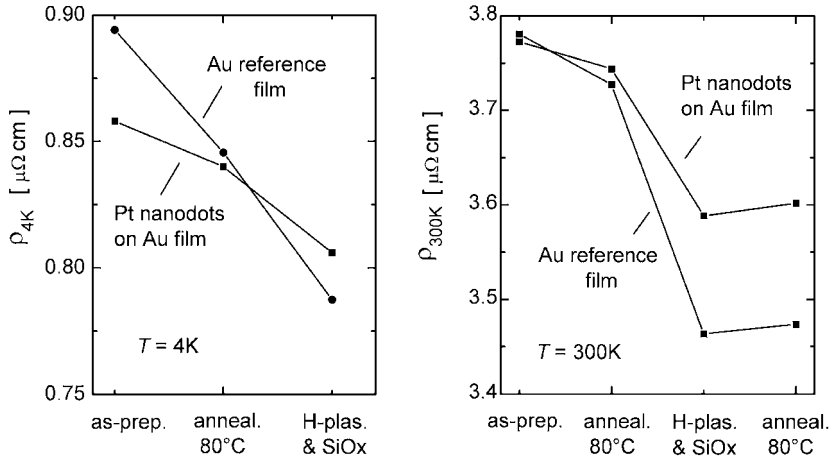

Figure 3. Resistivity at T = 4 K (left) and T = 300 K (right) of the Pt nanomodulated sample as compared to the reference film (thickness of both films: t = 25.4 nm). The resistivity of both samples decreases strongly with increasing surface cleanliness.

tivity $\rho_{300\,K}$ determined at T = 300 K of a nanomodulated Au film is compared with the values acquired from the corresponding Au reference film with both samples being treated simultaneously by the different preparational procedures. In the case of the as-prepared samples and the data taken in the cryostat without any additional treatments, the resistivity of the nanomodulated sample is found to be smaller than the reference film at both temperatures. This is opposite to what is expected for a nanomodulated sample, which should reveal a resistivity enhancement related to a smaller specularity parameter p due to the additional roughness induced by the nanoparticles.

In order to unravel whether adsorbates are responsible for this surprising result, in a first step, all samples were annealed within the cryostat to T = 80 °C for 3 days which is expected to remove the adsorbed water layer from the sample surface. After this procedure both, $\rho_{4\,K}$ and $\rho_{300\,K}$, are found to be reduced with the low temperature value of the reference film still being higher than the corresponding value measured for the nanomodulated film. In a second step, the sample surface was cleaned by removing all hydrocarbon adsorbates in a hydrogen plasma (5 min, 100 W, 0.01 mbar) as evidenced in Figure 2 (b) by means of a vanishing C-ls peak intensity followed by the in situ evaporation of an insulating layer (SiO), in order to protect the metallic film surface from re-adsorption of contaminants during sample transport under ambient conditions to the cryostat. Again, $\rho_{4\,K}$ as well as $\rho_{300\,K}$ are found to be significantly decreased as compared to the previous annealed state of the samples. Additionally and most gratifying, after this cleaning and protecting, the resistivity of the nanomodulated film is observed to be higher than the resistivity of the reference film for both temperatures which is consistent with the expected decrease of the specularity parameter p for the nanomodulated sample.

After carefully characterizing the resistivity as a function of temperature in this state of the samples, a further annealing cycle to T = 80 °C was performed. Since adsorbates/contaminants deposited by the ex situ preparation/transport should be located on top of the SiO protection layer rather than at the interface Au/SiO, in this case, no changes in resistivity are expected due to annealing. Such behavior can most notably be observed in Figure 3 within the experimental uncertainty. Thus, the addition of a protection layer after a hydrogen-plasma induced cleaning step allows for the analysis of the temperature-dependent resistivity $\rho(T)$ dominated by intrinsic surface scattering rather than by surface contaminations. Under these conditions, the influence of modulating a metal film surface by depositing an array of Pt nanoparticles on its electrical transport properties should be detectable.

Temperature Dependence of the Resistivity – Comparison with the FS Model

To determine the characteristic properties of a t = 25.4 nm Au film and to estimate the influence of the nanomodulation on its electrical properties, $\rho(T)$ was measured between 4 K and 300 K using the lock-in technique (Figure 4, open symbols) and the results were compared with the predictions of the classical size effect model of FS (Figure 4, solid lines). This was achieved by means of a numerical fitting procedure (for details see ref.[23,24]). The best fits to the experimental data have been added as solid lines to Figure 4 showing nearly perfect agreement between theory and experiment over the whole temperature range. While such a behavior has already been observed in previous studies on epitaxially grown Au films[23,24] it is rather surprising in the case of the nanomodulated film where deviations from the classical description are expected. On the other hand, after the more qualitative discussion of $\rho_{4\,K}$ and $\rho_{300\,K}$, as shown in Figure 3, the agreement between the experimental and theoretical results within the FS model legitimates extracting all relevant parameters e.g. the specularity parameter p, the electron mean-free path due to impurities l_{imp} and the Debye temperature θ_D. This allows a more detailed analysis of the electrical properties of the

nanomodulated sample as compared with the corresponding Au reference. The resulting sets of parameters are summarized in Table 1 as obtained for the as-prepared, the annealed, as well as the SiO covered state.

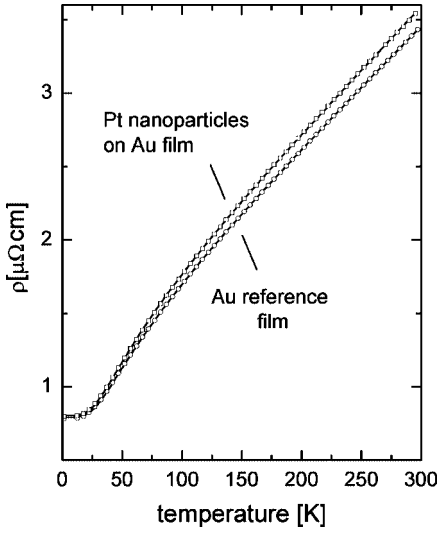

Figure 4. Temperature dependence of the resistivity of a Pt nanomodulated Au thin film sample as compared to the corresponding Au reference film (thickness of both films: t = 25 nm) after exposure to a hydrogen plasma and the in situ deposition of a SiO protection layer (open symbols). The solid lines represent the best fit to the experimental data using the FS model.

Table 1. FS fit parameters derived from the measured $\rho(T)$ curves of the Au reference sample and the nanomodulated sample in the as-prepared, the annealed and the SiO covered state.

	Au reference			Pt nanodots on Au		
	as-prep.	anneal.	SiO	as-prep.	anneal.	SiO
p	0.20	0.21	0.30	0.19	0.19	0.26
l_{imp} [nm]	700	819	697	854	905	805
θ_D [K]	185	190	178	189	191	184

For all measurements, the FS fit gives values for θ_D which are close to the bulk value of 184.6 K as obtained from fitting the temperature dependence of the resisitivity of Au bulk samples[36] with our fitting routine. The latter value itself agrees well with Debye temperatures deduced from resistivity measurements by other groups.[37,38] It is important to note that θ_D values for bulk Au extracted from transport measurements are found to be systematically larger than the corresponding values determined from XRD measurements by analyzing the temperature dependence of the Debye–Waller factor (165–170 K). This might be due to a different weighting of the real phonon density of states by the two different methods.

The similarity of the Debye temperatures extracted for the different states of the reference samples (as-prepared, annealed, SiO covered) confirms that the deposition of Pt nanoparticles on top of the epitaxially grown film using the micellar technique did not change its dynamic properties by, e.g., absorbing a significant amount of hydrogen during the hydrogen plasma treatment. This is also confirmed by analyzing l_{imp}, which determines the residual resistivity of the corresponding bulk material caused by impurities, grain boundaries or other lattice defects. This parameter remains roughly constant for both types of films (reference sample, nanomodulated sample) independent of the condition of the film surface (as-prepared, annealed, covered with SiO). In addition, the order of magnitude observed for l_{imp} in Table 1 also agrees well with the values observed for non-hydrogen plasma treated Au films of similar thickness, studied earlier.[23] Furthermore, the high value of about 800 nm observed for the electron mean free path due to impurities etc. of the corresponding (hypothetical) bulk material also confirms that the concentration of impurities is small and the grain size is large as compared to the sample thickness of t = 25 nm. This adds confidence that the Au films studied here can indeed be used as sensors for surface scattering processes (electron mean free path of the corresponding bulk material is much larger than the film thickness).

It is worth mentioning that by fitting the FS model to the temperature-dependent resistivity of a thin film, reasonable estimates can be extracted for the parameter l_{imp} describing the average distance between impurities or defects within the corresponding bulk material having the same morphology as the thin film. Thus, although the thin film resistivity is enhanced by surface scattering as compared to the bulk resistivity, the above analysis provides insight into the morphology of the thin film by means of impurity/defect concentrations, which is an important issue for the design of metallic interconnects[15,18] in microelectronics.

In Table 1, both parameters θ_D and l_{imp} do not vary significantly when the properties of the sample surface are changed. The appropriate quantity providing information on the condition of the sample surface (cleanliness and nanomodulation) is the specularity parameter p. For the as-prepared Au reference sample, the specularity parameter p = 0.203 is rather small. Only about one fifth of all electrons that contribute to the current are scattered specularly at the film surface or interface. As expected, p is slightly enhanced after moderate annealing of the sample in vacuo and p is increased further to 0.302 after removing all adsorbates by a hydrogen plasma and protecting the sample surface with a SiO layer. The probability of specular surface scattering is obviously significantly reduced by adsorbates on the film surface. Even though the probability of specular reflection is increased by almost 50% for the reference film due to an improved cleanliness at the surface, the absolute value of p is still rather small and only about 1/3 of all electrons are scattered specularly at the film surface or interface.

Once it is known that the specularity coefficient p of the Au reference sample is only 0.302 even in the best case, the effect of the Pt nanomodulation on the transport properties is expected to be comparatively small. To demonstrate the effect of modulating a Au surface by an array of Pt nanoparticles, the specularity coefficients p for the Au reference and the nanomodulated sample as extracted for the different surface conditions are summarized in Figure 5. In every case (as-prepared, annealed, SiO covered), the specularity coefficient p of the nanomodulated sample is

smaller than that of the Au reference. The reduction of p due to the nanomodulation is most pronounced when the nonmodulated reference Au film exhibits a high degree of specular reflection (SiO covered state). Thus, the main conclusion of the present work is that the decoration or nanomodulation of an otherwise optimized Au surface with arrays of Pt nanoparticles showing a high degree of hexagonal short-range order just reduces the probability of specular reflection, as would be expected for randomly distributed additional scatterers.

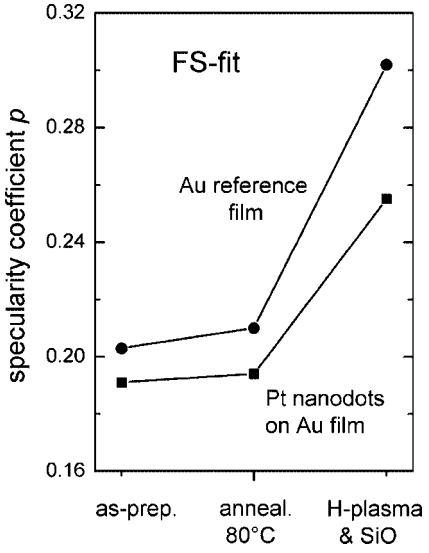

Figure 5. Specularity parameter p for the Au reference and the nanomodulated sample. By improving the surface cleanliness, p is enhanced. The nanomodulation generally leads to an increased probability of diffuse surface scattering as compared to the Au reference.

In order to better understand why diffuse surface/interface scattering dominates in the present experiment, the influence of the Nb seedlayer on electron transport has to be examined in more detail. Comparing the room temperature electrical resistivity of bulk Au (ρ = 2.2 μΩcm) and Nb (ρ = 15 μΩcm) and taking into account the different thickness of both materials (Nb: 1 nm, Au: 25.4 nm) it is obvious that electrical transport through the Nb layer can be neglected. The main impact of the seedlayer on the sample resistivity most likely is a change of the specularity parameter p at the interface between the Au film and the seedlayer as compared to a hypothetical interface between the Au film and the sapphire surface.

Investigations of specular electron scattering in Au films covered with 0.6 nm of Ta were observed to significantly increase the film resistivity by s–d scattering in contrast to Ag or Cu, which did not quench specular reflection.[11] Thus, it is very likely that scattering of the conduction electrons at the Au/Nb interface is not specular but rather diffuse. Unfortunately, this Nb seedlayer cannot be avoided if continuous, flat, epitaxially grown Au films are required as in our study. The only way to achieve Au films of similar quality is to use Fe or Cr seedlayers, which will worsen the conditions when compared with Nb because of the additional strong spin scattering at the interface, an effect which is well known, e.g., from magnetic (GMR) sensors.

Finally, it is worth mentioning, that Pt nanoparticles deposited directly onto the sapphire substrate before growing the Au film in order to avoid surface roughening induced by the plasma treatments did not result in an improved value of the specularity parameter p. Instead, l_{imp} of those films was found to be reduced to about 100 nm (as compared to 800 nm in the case of nanoparticles "on-top") probably due to a distorted epitaxial growth of the Au film on top of the Pt nanoparticles. For this sample configuration, an even further reduced specularity parameter was observed (0–0.1).

Conclusions

The influence of an array of Pt nanoparticles, prepared with a high degree of hexagonal short-range order on top of high quality epitaxial Au films on their electrical properties has been studied. It turned out that the temperature-dependent resistivity of the nanomodulated Au films are well described by the classical size effect model of Fuchs–Sondheimer. No indication could be detected that pointed to a specific effect of the nanoparticle array other than simply increasing the probability of diffuse surface scattering as would be expected for randomly distributed scatterers.

Experimental Section

Micellar Nanoparticles: Pt nanoparticle arrays were prepared using a method based on the self-assembly of suitable diblock-copolymers. A polystyrene(PS)-block-poly(2-vinylpyridine)(P2VP) copolymer was dissolved in an apolar solvent, where the copolymer chains assemble in spherical micellar objects with a hydrophilic P2VP core and a hydrophobic PS shell. The core of the micelle can be loaded with metal salts by adding the appropriate substance to the micellar solution. These metal salt loaded spherical micelles can easily be transferred onto substrates by dip coating, where, again by self-assembly, hexagonal arrays of micelles are formed. With the aid of a combined oxygen and hydrogen plasma process the micellar polymer can be removed, the metal salt can be reduced and spectroscopically clean arrays of metallic particles remain on the substrate. The hexagonal short-range order of the particles was not destroyed by the plasma process. Details on the preparation of micellar solutions and the plasma process can be found elsewhere.[26,27] For the work here, Pt nanoparticles were prepared with a diameter of about 3 nm and a spacing of about 32 nm.

Sample Preparation: The epitaxial Au films were prepared at about 300 °C on c-cut sapphire substrates with a 1 nm Nb seedlayer. The details are described in ref.[28] The samples are structured with standard photo lithography techniques and wet etching in I/KI solution[39] or etched in an RIE-plasma process (Oxford instruments, RIE-PlasmaLab 80Plus). The pattern is shown schematically in Figure 6. Twelve contacts allow four-probe measurements of the resistance on several segments of the sample.

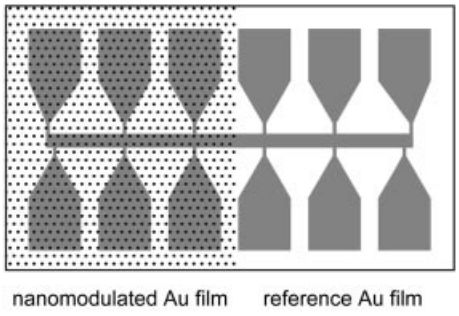

Figure 6. Sketch of a structured nanomodulated Au film sample. One half of the sample is covered with nanoparticles, the other serves as a reference. Four-probe measurements are possible on different segments on both sides.

In the size effect experiments, surface scattering properties of thin films were investigated by the temperature dependence of the resistivity and the specularity parameter p was determined by fitting to FS theory. For experiments on nanomodulated samples, one has to consider the ordinary size effect of thin films and the, probably, small influence of the nanomodulation. For this reason, both a nanomodulated Au film and a Au reference film are prepared in parallel on the same substrate as sketched in Figure 6. In this way, both films can be measured under identical conditions at the same time. All other processes (film growth, plasma exposure, lithography) were performed on the whole sample so that again both films undergo identical treatments and differ only by the nanomodulation. Such a relative measurement should enable the investigation of the influence of nanomodulation on thin film resistivity even if its effect is small.

The thickness of the epitaxial Au films was determined by means of a careful analysis of the Laue oscillations observed in the corresponding X-ray diffraction spectra using the program 'SUPREX'.[40,41] Because of the high quality of the films used in this study, an oscillating intensity could be observed over a wide range of angles covering the small angle as well as the large angle scattering regimes, respectively (for more details, see ref.[23]).

In order to control the chemical state of the Au surface and the Pt nanoparticles after the different preparational steps, the specimens were introduced into the analysis chamber of a commercial electron spectrometer (Fisons ESCALAB-210) and analyzed under ultrahigh vacuum conditions by means of XPS using monochromatized Al-K_α radiation ($h\nu$ = 1486.6 eV, spot size < 1 mm). Data were acquired using an overall energy resolution (electrons and photons) of between 0.5 and 1 eV, full width at half maximum (FWHM). At this point, it is important to note that by combining two separate chambers via a load-lock system, the plasma treatments and the XPS measurements could be performed in situ.

Acknowledgments

Financial support by the Deutsche Forschungsgemeinschaft (DFG) within SPP 1072 as well as SFB 569, the Swiss National Science Foundation (NF), and the NCCR "Nanoscale Science" is gratefully acknowledged.

[1] J. J. Thomson, *Proc. Cambridge Phil. Soc.* **1901**, *11*, 120.
[2] K. Fuchs, *Proc. Cambridge Phil. Soc.* **1938**, *34*, 100–108.
[3] E. H. Sondheimer, *Advan. Phys.* **1952**, *1*, 1–42.
[4] D. Schumacher, in: *Surface Scattering Experiments with Conduction Electrons* (Ed.: G. Holder), Springer Tracts in Modern Physics, Springer, Berlin, **1993**, vol. 128.
[5] S. B. Soffer, *J. Appl. Phys.* **1967**, *38*, 1710–1715.
[6] U. Jacob, J. Vancea, H. Hoffmann, *Phys. Rev. B* **1990**, *41*, 11852–11857.
[7] G. Reiss, E. Hastreiter, H. Brückl, J. Vancea, *Phys. Rev. B* **1991**, *43*, 5176–5179.
[8] G. Reiss, H. Brückl, *Surf. Sci.* **1992**, *270*, 772–776.
[9] J. Ederth, L. B. Kish, E. Olsson, *Phys. Rev. B* **1995**, *51*, 17116–17130.
[10] A. L. Cabrera, W. Garrido-Molina, E. Morales-Leal, J. Espinosa-Gangas, I. K. Schuller, D. Lederman, *Langmuir* **1998**, *14*, 3249–3254.
[11] W. F. Egelhoff, Jr., P. J. Chen, C. J. Powell, D. Parks, G. Serpa, R. D. McMichael, D. Martien, A. E. Berkowitz, *J. Vac. Sci. Technol. B* **1999**, *11*, 1702–1707.
[12] J. Ederth, L. B. Kish, E. Olsson, C. G. Granqvist, *J. Appl. Phys.* **2000**, *88*, 6578–6582.
[13] H. D. Liu, Y. P. Zhao, G. Ramanath, S. P. Murarka, G. C. Wang, *Thin Solid Films* **2001**, *384*, 151–156.
[14] G. Palasantzas, J. T. de Hosson, *Phys. Rev. B* **2001**, *63*, 125404.
[15] R. M. Patrikar, C. Y. Dong, W. J. Zhuang, *Microelectron. J.* **2002**, *33*, 929–934.
[16] O. Pfenningstorf, A. Petkova, Z. Kallassy, M. Henzler, *Eur. Phys. J. B* **2002**, *30*, 111–115.
[17] S. U. Jen, C. C. Yu, C. H. Liu, G. Y. Lee, *Thin Solid Films* **2003**, *434*, 316–322.
[18] C. U. Kim, J. Park, N. Michael, P. Gillespie, R. Augur, *J. Electron. Mater.* **2003**, *32*, 982–987.
[19] I. Vilfan, H. Pfnür, *The European Physical Journal B* **2003**, *36*, 281–287.
[20] S. M. Rossnagel, T. S. Kuan, *J. Vac. Sci. Technol. B* **2004**, *22*, 240–247.
[21] H. Marom, M. Eizenberg, *J. Appl. Phys.* **2004**, *96*, 3319–3323.
[22] R. A. Patrikar, *J. Appl. Surf. Sci.* **2004**, *228*, 213–220.
[23] G. Kästle, H.-G. Boyen, A. Schroder, A. Plettl, P. Ziemann, *Phys. Rev. B* **2004**, *70*, 165414–165419.
[24] G. Kästle, T. Müller, H.-G. Boyen, A. Klimmer, P. Ziemann, *J. Appl. Phys.* **2004**, *96*, 7272–7277.
[25] J. M. Camacho, A. I. Oliva, *Microelectron. J.* **2005**, *36*, 555–558.
[26] J. P. Spatz, S. Mössmer, C. Hartmann, M. Möller, T. Herzog, M. Krieger, H.-G. Boyen, P. Ziemann, B. Kabius, *Langmuir* **2000**, *16*, 407.
[27] G. Kästle, H.-G. Boyen, F. Weigl, G. Lengl, T. Herzog, P. Ziemann, S. Riethmüller, O. Mayer, C. Hartmann, J. P. Spatz, M. Möller, M. Ozawa, F. Banhart, M. G. Garnier, P. Oelhafen, *Adv. Funct. Mater.* **2003**, *13*, 853–861.
[28] G. Kästle, H.-G. Boyen, B. Koslowski, A. Plettl, F. Weigl, P. Ziemann, *Surf. Sci.* **2002**, *498*, 168–174.
[29] B. Koslowski, H.-G. Boyen, C. Wilderotter, G. Kästle, P. Ziemann, R. Wahrenberg, P. Oelhafen, *Surf. Sci.* **2001**, *475*, 1–10.
[30] A. Relitzki, A. Hilger, H. Hovel, U. Kreibig, D. Schumacher, H. Winkes, in: *Science and Technology of atomically engineered materials* (Ed.: P. Jena), World Scientific, **1998**, p. 453.
[31] Landolt-Börnstein, *Group III* ("Condensed Matter"), vol. 26 ("Diffusion in Solid Metals and Alloys"), Springer, Berlin, **1990**.
[32] G. K. Wertheim, P. H. Citrin, *J. Electron Spectrosc. Relat. Phenom.* **1985**, *37*, 57–67.
[33] S. Doniach, M. Sunjic, *J. Phys. C* **1970**, *3*, 285–291.
[34] N. Z. Negm, L. M. Watson, P. R. Norris, A. Szasz, *J. Phys. F: Met. Phys.* **1987**, *17*, 2295–2301.
[35] G. K. Wertheim, P. H. Citrin, *Topics Appl. Phys.* **1978**, *26*, 197–206.
[36] J. Mydosh, P. Ford, M. Kawatra, T. Whall, *Phys. Rev. B* **1974**, *10*, 2845–2856.
[37] J. Jacobs, R. Birtcher, R. Peacock, *J. Vac. Sci. Technol. B* **1969**, *7*, 339.

[38] N. Karpe, G. Lapogian, J. Bottiger, J. Krog, *Philos. Mag. B* **1995**, *71*, 445.
[39] W. Eidelloth, R. L. Sandstrom, *Appl. Phys. Lett.* **1991**, *59*, 1632–1634.
[40] E. E. Fullerton, J. Guimpel, O. Nakamura, I. K. Schuller, *Phys. Rev. Lett.* **1992**, *69*, 2859–2862.
[41] E. E. Fullerton, I. K. Schuller, H. Vanderstraeten, Y. Bruynseraede, *Phys. Rev. B* **1992**, *45*, 9292–9310.

Received: June 6, 2005
Published Online: August 17, 2005

